

Effects of Al doping on the normal and superconducting properties of MgB₂: A specific heat study

M. Putti,¹ M. Affronte,² P. Manfrinetti,³ and A. Palenzona³¹*INFM-LAMIA, CNR-IMEM and Dipartimento di Fisica, Università di Genova, via Dodecaneso 33, 16146 Genova, Italy*²*INFM-S³ National Research Center on nanoStructures and bioSystems at Surfaces and Dipartimento di Fisica, Università di Modena e Reggio Emilia, via G. Campi 213/A, I-41100 Modena, Italy*³*INFM-LAMIA and Dipartimento di Chimica e Chimica Industriale, Università di Genova, via Dodecaneso 31, 16146 Genova, Italy*

(Received 22 February 2003; revised manuscript received 23 May 2003; published 23 September 2003)

The effects of Mg substitution by Al on the specific heat of MgB₂ have been studied in the normal and in the superconducting state. The Sommerfeld coefficient, evaluated by measurements in magnetic field up to 7 T, progressively decreases from $\gamma = 3.0 \pm 0.2$ mJ/mol K² for undoped MgB₂ down to $\gamma = 1.9 \pm 0.2$ mJ/mol K² for Mg_{0.6}Al_{0.4}B₂ as a result of the change of the density of states and of the electron-phonon coupling constants. The superconducting contribution to the specific heat c_{sc} clearly shows an excess at low temperature compared with conventional single-gap BCS behavior also for doped samples with x up to 0.3. The two-band model has been used to fit the temperature dependence of c_{sc} and the amplitude of the two gaps has been evaluated for different Al concentrations. The changes of the energy gaps are in a rather poor agreement with those predicted by taking into account changes in the electronic and phononic structure only. We suggest that disorder also plays an important role when Al substitutes Mg.

DOI: 10.1103/PhysRevB.68.094514

PACS number(s): 74.70.Ad, 74.25.Bt, 74.62.Dh

I. INTRODUCTION

Two years after the discovery of superconductivity in magnesium diboride¹ there is a general consensus about the nature of superconductivity in this compound. The observation of the isotope effect² and the dependence of the critical temperature T_c on pressure³ soon provided evidences for phonon mediated pairing mechanism, although results of many experiments were not consistent with a conventional strong-coupling BCS scenario. To explain the behavior of critical fields, specific heat, and tunneling, a two-gap model was thus invoked. Two band sets cross the Fermi level in MgB₂: two σ bands derived from the $p_{x,y}$ boron states and two π bands derived from the p_z boron states. These electronic bands have very different character, the σ bands being of hole type and nearly two-dimensional (2D) while the 3D π bands are essentially of electron type. Two distinctive superconducting gaps, Δ_σ and Δ_π , can actually be associated to the σ and π bands.^{4,5} Although this scenario offers a simple explanation for some superconducting properties,⁶⁻⁸ the effects on T_c of the interplay of these two bands still need to be clarified.

The Al substitution of Mg acts as an electron doping. Precise band-structure calculations on the effects of Al doping have been proposed⁹ and these still need to be supported by experimental results. Due to the different size of Al ion with respect to Mg, other effects of the Al doping are the change of the phonon spectrum, in particular the stiffening of the E_{2g} mode, and the increase of disorder that gives rise to intraband and interband relaxation rates modifying the coupling between the bands. The progressive loss of superconductivity with increasing Al doping is discussed in literature in terms of the σ band filling^{9,10} and the stiffening of the E_{2g} mode which decreases the electron-phonon coupling,¹¹⁻¹³ but open questions are how the gap structure and the interband coupling vary with the increase of impurity and to

which extent the two-gap model can be used for such a compound.

In this paper we present a systematic study of specific heat performed on high quality polycrystalline Mg_{1-x}Al_xB₂ samples. The electronic specific heat in the normal and the superconducting state has been analyzed within the two-band model. Results allow us to monitor the variation of the Sommerfeld constant and superconducting energy gaps with Al doping.

II. SAMPLE PREPARATION AND EXPERIMENTAL TECHNIQUES

Polycrystalline powders were prepared by mixing stoichiometric proportions of the commercial pure elements (purity 99.99%, 99.999%, and 99.7% for Mg, Al, and B, respectively), closed in Ta crucibles sealed under argon and reacted at 1000 °C for 150 h in quartz tubes under vacuum. X-ray diffraction patterns show that our samples are single-phase AlB₂ type for all the Al concentrations in agreement with previous report.¹² No traces of the phase separation for $0.1 < x < 0.25$ reported in Ref. 14 were found: the long annealing we used is probably needed in order to obtain single-phase material.¹⁵ A moderate Bragg peak broadening may indicate a degree of inhomogeneity in the local Al concentration. Lattice parameters are reported in Table I and they

TABLE I. Lattice parameters of Mg_{1-x}Al_xB₂ as a function of the Al concentration x .

x	a (Å)	c (Å)
0	3.085(1)	3.525(1)
0.1	3.080(1)	3.483(1)
0.2	3.077(1)	3.462(1)
0.3	3.069(1)	3.425(1)
0.4	3.064(1)	3.398(1)

follow a linear variation with x . Heat-capacity measurements were performed by a commercial Quantum Design PPMS-7T system which makes use of the relaxation method. Preliminary measurements of the bare calorimeter with 0.2 mg of Apiezon N grease were performed in different magnetic fields in order to extract the contribution of *addenda*. Samples having mass ranging from 10 to 20 mg were cut from pellets further sintered at 1000 °C for 15 days.

III. RESULTS

The temperature dependence of the specific heat c from 2 to 300 K of $Mg_{1-x}Al_xB_2$ samples with $x=0, 0.1, 0.2, 0.3,$ and 0.4 is reported in Fig. 1. At high temperatures the molar specific heat curves of samples with different Al concentrations almost overlap each other, unlike what occurs for different substitutions. This suggests that effects of Al substitution on the lattice are not drastic. Differences in the specific heat behavior are clearly evident at low temperature where a spreading of one order of magnitude in the curves with different Al concentration is present; the behavior is not monotone, in fact, in respect to the pure compound, at 2 K the molar specific heat decreases for $x=0.1$ and then increases for larger doping. Many factors determine the low-temperature specific heat (Sommerfeld constant, Debye temperature, critical temperature, gap amplitudes, etc.), and to separate these effects in the following we shall focus our analysis on data below 40 K. For each Al concentration we performed a set of measurements between 2 and 40 K and in magnetic field of 0, 3, 5, and 7 T. Results are plotted as c/T vs T^2 in Fig. 2 in which, for the sake of clarity, we plot only data in zero field and 7 T. The superconducting contributions can be easily visualized by comparing data in zero field with those obtained in magnetic field: the jump at T_c is well pronounced in undoped MgB_2 and it gets broader as the Al concentration increases. The critical temperature was defined at half the specific heat anomaly and the error bar takes into account the transition amplitude; the dependence of T_c to the Al concentration x is reported in Table II. T_c decreases linearly in reasonable agreement with literature data,^{12,16} but the few points and the large error bars do not allow us to

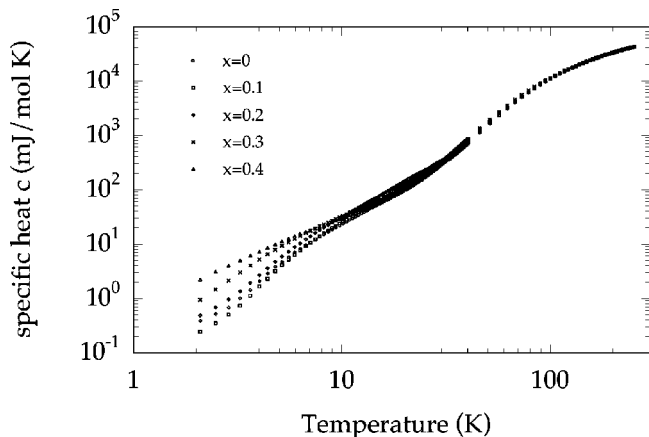


FIG. 1. Specific heat of $Mg_{1-x}Al_xB_2$ with $x=0, 0.1, 0.2, 0.3,$ and 0.4 from 2 to 300 K.

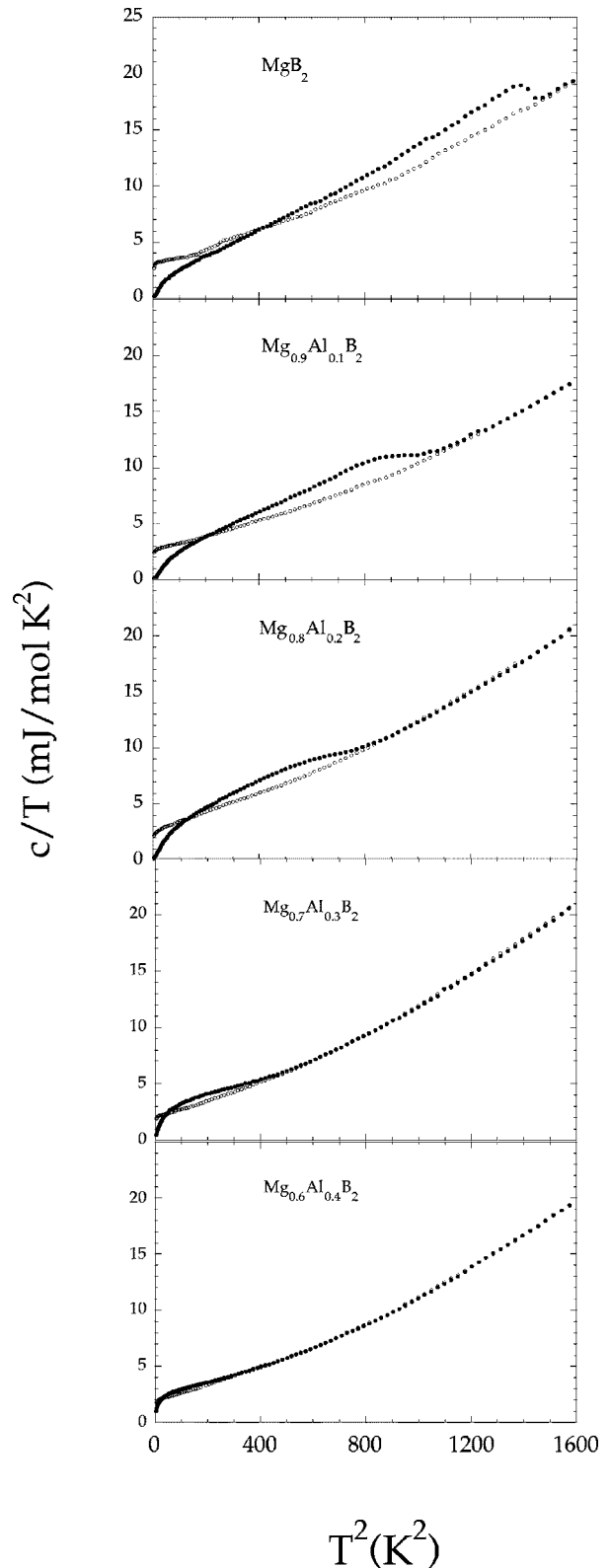


FIG. 2. Low-temperature specific heat of $Mg_{1-x}Al_xB_2$ with $x=0, 0.1, 0.2, 0.3,$ and 0.4 plotted as c/T vs T^2 . For the sake of clarity, only measurements in zero field (filled circles) and in 7 T (open circles) are reported for each sample.

TABLE II. Critical temperature T_c , γ (Sommerfeld constant), β , and δ coefficients of the $c(H=7\text{ T}) = \gamma T + \beta T^3 + \delta T^5$ fitting curve, and Debye temperature Θ_D for different Al concentrations x in $\text{Mg}_{1-x}\text{Al}_x\text{B}_2$.

x	T_c (K)	γ (mJ/mol K ²)	β (mJ/mol K ⁴)	δ (mJ/mol K ⁶)	Θ_D (K)
0	38.0 ± 0.3	3.00 ± 0.2	$(6.4 \pm 0.2) \times 10^{-3}$	$(2.4 \pm 0.2) \times 10^{-6}$	670 ± 15
0.1	31 ± 1.5	2.80 ± 0.2	$(4.8 \pm 0.2) \times 10^{-3}$	$(2.9 \pm 0.2) \times 10^{-6}$	740 ± 15
0.2	25 ± 2	2.55 ± 0.2	$(7.2 \pm 0.2) \times 10^{-3}$	$(2.7 \pm 0.2) \times 10^{-6}$	650 ± 15
0.3	18 ± 2	2.10 ± 0.2	$(6.2 \pm 0.2) \times 10^{-3}$	$(3.6 \pm 0.2) \times 10^{-6}$	680 ± 15
0.4	12 ± 2.5	1.90 ± 0.2	$(5.9 \pm 0.2) \times 10^{-3}$	$(3.3 \pm 0.2) \times 10^{-6}$	690 ± 15

observe the change of slope around $x=0.3$ as previously emphasized.¹²

For MgB_2 , the linear term of the specific heat in a magnetic field includes both the Sommerfeld constant γ and a mixed state contribution, yet Bouquet and co-workers^{17,18} demonstrated that the intercept of the c/T vs T^2 curve rapidly saturates (already at $H_{c2}/2$) as the magnetic field increases. The normal-state Sommerfeld constant γ can be thus defined extrapolating the intercept of the c/T vs T^2 curves to the high-field regime. For Al-doped MgB_2 this definition is very close to the value of the intercept of the c/T vs T^2 curve in 7 T since the upper critical field $H_{c2}(0)$ decreases as the Al concentration increases.¹⁶ A close data inspection also reveals that Schottky anomalies are very small for our samples at least for $T > 2$ K. The Sommerfeld constants γ thus estimated are reported in Table II and plotted in Fig. 3 as a function of the Al concentration x . We found that γ progressively decreases from 3.0 ± 0.2 mJ/mol K² for undoped MgB_2 to 1.9 ± 0.2 mJ/mol K² for $\text{Mg}_{0.6}\text{Al}_{0.4}\text{B}_2$. As soon as the normal-state γ value was obtained, the temperature dependence of the normal-state specific heat from T_c up to 40 K in 7 T were fitted with a curve $c(H=7\text{ T}) = \gamma T + \beta T^3 + \delta T^5$. Results are reported in Table II for each Al concentration. The β value is equal to $\beta[\text{mJ/mol K}^4] = 1944/\Theta_D(\text{K})^3$ within the framework of the Debye model and in the limit of low temperature, while the δT^5 term was introduced as a high-temperature correction to the T^3 Debye

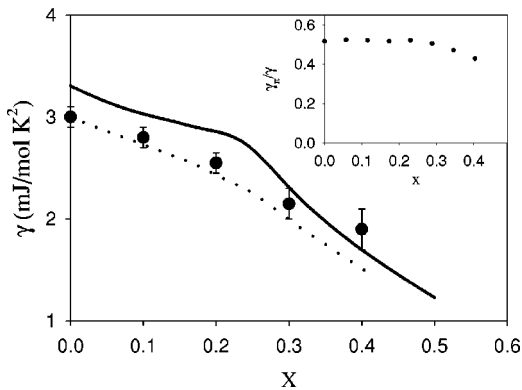


FIG. 3. The normal-state Sommerfeld coefficient γ as a function of the Al concentration x (circles are values evaluated from our specific heat experiments). The calculated γ coefficients are taken from Ref. 13 (continuous line) and Ref. 24 (dotted line). Inset shows the partial contribution γ_π/γ due to the π band evaluated from Ref. 24.

law. The x dependence of Θ_D is shown in Table II.

The superconducting contribution c_{sc} is then estimated as $c_{sc} = c(H=0) - [\beta T^3 + \delta T^5]$. The entropy difference $\Delta S = \int (c_{sc}/T - \gamma) dT$ between the superconducting- and the normal-state contribution was evaluated and we were able to verify that ΔS actually vanishes close to T_c . For $x=0.4$ the superconducting contribution is so small and the transition is so broad to prevent any quantitative analysis, this is the reason why in the following we limit the discussion of the superconducting state to x up to 0.3. For undoped MgB_2 our results can be compared with those reported in literature: we found $\gamma = 3.0 \pm 0.2$ mJ/mol K² and $\beta = (6.4 \pm 0.1) \times 10^{-3}$ mJ/mol K⁴ which are very close to those reported in Refs. 17, 19, and 20. The normalized superconducting contributions to specific heat $c_{sc}/t\gamma T_c$ of $\text{Mg}_{1-x}\text{Al}_x\text{B}_2$ are plotted as a function of reduced temperature $t = T/T_c$ in Fig. 4 for $x=0, 0.1, 0.2$, and 0.3 . Note that, for undoped MgB_2 the jump $[c_{sc} - \gamma T_c]/t\gamma T_c = 0.87$ at T_c and the shape of $c_{sc}/t\gamma T_c$ vs t with the excess of $c_{sc}/t\gamma T_c$ at $\sim T_c/4$ are very close to that reported in literature.^{17,19,20} An interesting result is the fact that the excess of c_{sc} with respect to a conventional BCS behavior is also observed in $\text{Mg}_{1-x}\text{Al}_x\text{B}_2$ with $x=0.1, 0.2$, and 0.3 , and this is an important feature that will be used in the following data analysis. Similar features were also observed in damaged²¹ and carbon doped²² MgB_2 .

IV. DATA ANALYSIS AND DISCUSSION

We first consider the normal-state electronic contribution $c_{el} = \gamma T$ to the specific heat and its dependence on the Al content. For a two-band system the Sommerfeld constant γ can be expressed as²³

$$\gamma = \gamma_\sigma + \gamma_\pi,$$

where

$$\gamma_\sigma = \frac{2}{3} \pi^2 k_B^2 N_\sigma (1 + \lambda_{\sigma\sigma} + \lambda_{\sigma\pi})$$

and

$$\gamma_\pi = \frac{2}{3} \pi^2 k_B^2 N_\pi (1 + \lambda_{\pi\pi} + \lambda_{\pi\sigma}).$$

N_σ and N_π are the densities of states of the σ and π bands, respectively, and $\lambda_{\sigma\sigma}$, $\lambda_{\sigma\pi}$, $\lambda_{\pi\pi}$, and $\lambda_{\pi\sigma}$ are the electron-phonon coupling constants. The Al doping modifies the structural and electronic properties of MgB_2 and consequently the densities of states;^{9,13,24} moreover it changes the phonon spectrum, in particular there is a stiffening of the E_{2g} mode, and the electron-phonon coupling constants are ex-

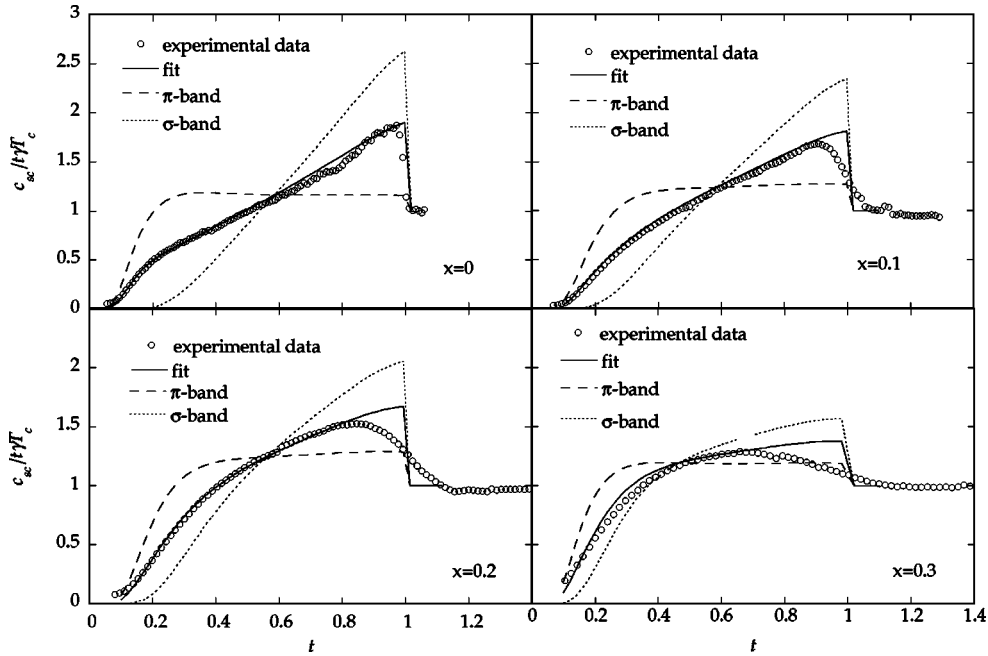


FIG. 4. The normalized superconducting contribution to specific heat $c_{sc}/t\gamma T_c$ of $\text{Mg}_{1-x}\text{Al}_x\text{B}_2$ plotted as a function of reduced temperature $t=T/T_c$ (circles) for $x=0, 0.1, 0.2$, and 0.3 . Continuous lines are the best fit of data with the two-gap model.

pected to vary.^{13,24} In Fig. 3 we plot γ values as a function of the Al doping. The continuous and the dotted lines represent the values calculated in Ref. 13 and Ref. 24, respectively, by introducing the partial densities of states N_σ and N_π and the coupling constants as a function of the Al doping. There is a reasonable agreement between experimental and theoretical calculations, both in absolute value and in the x dependence. We point out that the partial densities of states do not differ too much in the two calculations while the coupling constants are obtained in different ways: Profeta and co-workers¹³ take into account the E_{2g} mode only, while Bussmann-Holder and Bianconi²⁴ calculate the coupling constants by reversing the McMillan equation. With the density of states and the coupling constants of Ref. 24 we can plot γ_π/γ as a function of x (see inset of Fig. 3). It turns out that this ratio is ~ 0.5 up to $x=0.3$, i.e., the partial contributions of σ and π bands to the normal-state specific heat remain essentially constant and nearly equal as the Al doping increases.

As noted in the preceding section, the specific heat in the superconducting state shows an excess at low temperatures compared to the conventional single-gap BCS behavior (see Fig. 4). This leads us to analyze the $c_{sc}/t\gamma T_c$ vs t of Al doped MgB_2 in terms of the two-gap model proposed in Ref. 6. To which extent the two-gap model can be applied to $\text{Mg}_{1-x}\text{Al}_x\text{B}_2$ will be discussed below. Within this phenomenological model, the σ and π bands, characterized by a large $\Delta_\sigma(0)$ and a small $\Delta_\pi(0)$ gap, respectively, contribute to the specific heat proportionally to the fraction γ_σ/γ and γ_π/γ , respectively. Assuming a BCS-like temperature dependence for each gap as described in Ref. 6, the $c_{sc}/t\gamma T_c$ vs t curves can be fitted by adjusting three parameters: $\alpha_\sigma = \Delta_\sigma(0)/k_B T_c$, $\alpha_\pi = \Delta_\pi(0)/k_B T_c$, and $\chi = \gamma_\pi/\gamma_n$.

In Fig. 4 we plot $c_{sc}/t\gamma T_c$ vs t for $x=0, 0.1, 0.2$, and 0.3

with the best-fit curves whose parameters are summarized in Table III. For the undoped MgB_2 the data fit is excellent: $\alpha_\sigma \approx 1.88 \pm 0.05$, $\alpha_\pi \approx 0.58 \pm 0.02$, and $\chi \approx 0.5$ – 0.55 . Note that α_σ and α_π correspond to gap values which are in agreement with tunneling results²⁵ and the $\gamma_\pi \sim \gamma_\sigma$ ratio agrees well with theoretical calculations (see Fig. 3). For $x=0.1$ and 0.2 , the fit is still good even if, as the doping increases, the transition gets broader. For $x=0.3$, the two-band model fits less perfectly the experimental curve, but since an excess of specific heat for $t \leq 0.2$ is still present, an estimation of two gaps with a large error bar is given. It is worth pointing out that the reduced gaps α_σ and in particular α_π are well defined by the fitting procedure while, for the doped samples, χ can range from 0.4 to 0.55 without valuable changes in the quality of the fit. Therefore, we fix $\chi=0.5$ (the value expected from calculations, see Fig. 3) and evaluate the accuracy of the α_σ and α_π values by considering the change of these parameters as χ ranges from 0.45 to 0.55 and the critical temperature varies within T_c and its error bar.

Figure 5 (upper panel) shows $\Delta_\sigma(0)$ and $\Delta_\pi(0)$ as a function of the Al doping. $\Delta_\sigma(0)$ linearly decreases, while $\Delta_\pi(0)$ remains constant up to $x=0.2$. Therefore, $\Delta_\sigma(0)$ and $\Delta_\pi(0)$, which differ by more than a factor of 3 in pure MgB_2 , get closer as x increases. Similar behavior of $\Delta_\sigma(0)$ and $\Delta_\pi(0)$

TABLE III. Energy gap of $\text{Mg}_{1-x}\text{Al}_x\text{B}_2$ as a function of the Al concentration x . The error bars represent the accuracy in the determination of the α coefficients from the fitting procedure.

x	α_σ	α_π	$\Delta_\sigma(0)$ (meV)	$\Delta_\pi(0)$ (meV)
0	1.88 ± 0.05	0.58 ± 0.02	6.2 ± 0.1	1.90 ± 0.03
0.1	1.65 ± 0.1	0.75 ± 0.05	4.4 ± 0.2	2.02 ± 0.06
0.2	1.4 ± 0.2	0.8 ± 0.05	3.1 ± 0.3	1.7 ± 0.2
0.3	1.1 ± 0.3	0.6 ± 0.3	1.7 ± 0.5	1.0 ± 0.5

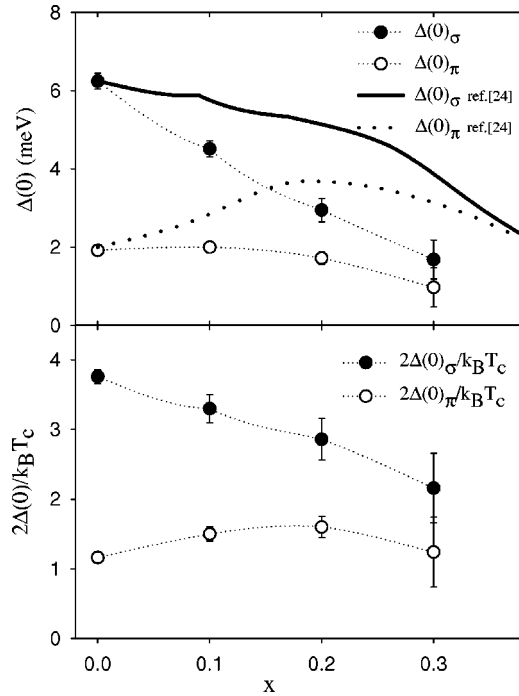


FIG. 5. Upper panel: superconducting gaps $\Delta_{\sigma}(0)$ and $\Delta_{\pi}(0)$ measured in $\text{Mg}_{1-x}\text{Al}_x\text{B}_2$ for different Al concentrations. Lines are theoretical expectations evaluated by taking into account band filling effects and changes in the electron-phonon coupling (from Ref. 24, normalized to the gap values of the pure compound). Lower panel: reduced gaps, $2\Delta_{\sigma}(0)/k_B T_c$ and $2\Delta_{\pi}(0)/k_B T_c$ plotted for different Al concentrations.

as a function of the Al doping has been recently observed in single crystals.²⁶

An evaluation of the gap amplitude as a function of the Al doping is given by Bussmann-Holder and Bianconi,²⁴ who considered the effects of density of states and electron-phonon coupling: there is only a qualitative agreement between the theoretical prediction and the experimental data. This comparison suggests that the changes in the electronic and phononic structure do not completely account for the changes in the energy gaps. Recently, Erwin and Mazin²⁷ predicted that Al impurities can increase the interband scattering to measurable levels. Therefore, the loss of superconductivity due to Al doping is a combination of different changes in the density of states, in the electron-phonon coupling, and in the interband scattering rate, and a quantitative analysis of experimental results requires the precise knowledge of all these effects.

The effects of impurity scattering in a two-gap superconductor was considered by Golubov and Mazin,²⁸ who evidenced that interband scattering by nonmagnetic impurities

has a pair-breaking effect and suppresses T_c as scattering by magnetic impurities does in a regular superconductor. The two gaps vary as interband scattering rate increases: in the weak scattering limit the larger gap rapidly decreases, while the small gap grows as a consequence of the fact that a larger number of pairs is scattered in the second band. The strong scattering limit is achieved when interband scattering rate becomes larger than the relevant phonon frequency. In the superstrong scattering regime T_c saturates to a limiting value, which is the critical temperature calculated in the fully isotropic BCS theory (19 K for MgB_2 , Ref. 5), and the two gaps merge to one, the isotropic BCS gap.

The reduced gaps plotted as a function of x in Fig. 5 (lower panel) show a behavior similar to those predicted in the weak scattering limit. Actually, if in the isotropic limit the BCS value 3.56 has to be reached, the reduced π gap seems to be still very small. Similar results were found by Wang *et al.*²¹ in irradiated MgB_2 samples and in carbon doped MgB_2 samples.^{22,29} In all these cases, although T_c was not far from the isotropic value, a two-gap feature was still present and $2\Delta_{\pi}(0)/k_B T_c$ values lower than 2 were found. Therefore, the evolution of the gaps with the disorder can be explained only qualitatively by the two-gap model and a close examination of the changes in the density of states as the interband scattering increases should be important for a deeper understanding of this topic.

In conclusion, we measured the changes of Sommerfeld coefficient γ of the normal-state specific heat due to Al doping in $\text{Mg}_{1-x}\text{Al}_x\text{B}_2$ with x up to 0.4. The changes of the density of states and of the electron-phonon coupling constants account rather well for the decrease of γ as Al content increases, and this is a direct proof of the doping effect introduced by Al in MgB_2 . We have also studied in detail the evolution of the superconducting contribution c_{sc} to specific heat in $\text{Mg}_{1-x}\text{Al}_x\text{B}_2$. For x up to 0.3, c_{sc} vs T shows an excess at low T with respect to the conventional BCS behavior, similar to what is observed in undoped MgB_2 . The c_{sc} vs T data fit well the curves obtained within the framework of a two-gap model, and this allowed us to estimate the evolution of the separated gaps Δ_{σ} and Δ_{π} as a function of the Al doping up to $x=0.3$. Changes in the electronic and phononic structure do not completely account for the evolution of the energy gaps and we believe that also disorder effects induced by the Al doping have to be considered.

ACKNOWLEDGMENTS

This work was partially supported by the Istituto Nazionale per la Fisica della Materia through the PRA UMBRA. The authors thank G. Profeta, A. Continenza, and S. Massidda for fruitful discussions.

¹J. Nagamatsu, N. Nakagawa, T. Muranaka, Y. Zenitani, and J. Akimitsu, *Nature (London)* **410**, 63 (2001).

²S.L. Bud'ko, G. Lapertot, C. Petrovic, C.E. Cunningham, N. Anderson, and P.C. Canfield, *Phys. Rev. Lett.* **86**, 1877 (2001).

³B. Lorenz, R.L. Meng, and C.W. Chu, *Phys. Rev. B* **64**, 012507 (2001).

⁴A.Y. Liu, I.I. Mazin, and J. Kortus, *Phys. Rev. Lett.* **87**, 087005 (2001).

- ⁵H.J. Choi, D. Roundy, H. Sun, M.L. Cohen, and S.G. Louie, *Phys. Rev. B* **66**, 020513 (2002).
- ⁶F. Bouquet, Y. Wang, R.A. Fisher, D.G. Hinks, J.D. Jorgensen, A. Junod, and N.E. Phillips, *Europhys. Lett.* **56**, 856 (2001).
- ⁷A. Brinkman, A.A. Golubov, H. Rogalla, O.V. Dolgov, J. Kortus, Y. Kong, O. Jepsen, and O.K. Andersen, *Phys. Rev. B* **65**, 180517(R) (2002).
- ⁸M. Putti, V. Braccini, E. Galleani D'Agliano, F. Napoli, I. Pallecchi, A.S. Siri, P. Manfrinetti, and A. Palenzona, *Phys. Rev. B* **67**, 064505 (2003).
- ⁹O. de la Pena, A. Aguayo, and R. de Coss, *Phys. Rev. B* **66**, 012511 (2002).
- ¹⁰A. Bianconi, S. Agrestini, D. Di Castro, G. Campi, G. Zangari, N.L. Saini, A. Saccone, S. De Negri, M. Giovannini, G. Profeta, A. Continenza, G. Satta, S. Massidda, A. Cassetta, A. Pifferi, and M. Colapietro, *Phys. Rev. B* **65**, 174515 (2002).
- ¹¹B. Renker, K.B. Bohnen, R. Heid, D. Ernst, H. Schober, M. Koza, P. Adelman, P. Schweiss, and T. Wolf, *Phys. Rev. Lett.* **88**, 067001 (2002).
- ¹²P. Postorino, A. Congeduti, P. Dore, A. Nucara, A. Bianconi, D. Di Castro, S. De Negri, and A. Saccone, *Phys. Rev. B* **65**, 020507 (2001).
- ¹³G. Profeta, A. Continenza, and S. Massidda, *Phys. Rev. B* (to be published).
- ¹⁴J.S. Slusky, N. Rogado, K.A. Regan, M.A. Hayward, P. Khalifah, T. He, K. Inumaru, S.M. Loureiro, M.K. Haas, H.W. Zandbergen, and R.J. Cava, *Nature (London)* **410**, 908 (2001).
- ¹⁵S. Serventi, G. Allodi, C. Bucci, R. De Renzi, G. Guidi, E. Pavarini, A. Palenzona, and P. Manfrinetti, *Phys. Rev. B* **67**, 134518 (2003).
- ¹⁶J.Y. Xiang, D.N. Zheng, J.Q. Li, L. Li, P.L. Lang, H. Chen, C. Dong, G.C. Che, Z.A. Ren, H.H. Qi, H.Y. Tian, Y.M. Ni, and Z.X. Zhao, *Phys. Rev. B* **65**, 214536 (2002).
- ¹⁷F. Bouquet, R.A. Fisher, N.E. Phillips, D.G. Hinks, and J.D. Jorgensen, *Phys. Rev. Lett.* **87**, 047001 (2001).
- ¹⁸F. Bouquet, Y. Wang, I. Sheikin, T. Plackowski, A. Junod, S. Lee, and S. Tajima, *Phys. Rev. Lett.* **89**, 257001 (2002).
- ¹⁹Y. Wang, T. Plackowski, and A. Junod, *Physica C* **355**, 179 (2001).
- ²⁰H.D. Yang, J.-Y. Lin, H.H. Li, F.H. Hsu, C.J. Liu, S.-C. Li, R.-C. Yu, and C.-Q. Jin, *Phys. Rev. Lett.* **87**, 167003 (2001).
- ²¹Y. Wang, F. Bouquet, I. Sheikin, P. Toulemonde, B. Revaz, M. Eisterer, H.W. Weber, J. Hinderer, and A. Junod, *J. Phys.: Condens. Matter* **15**, 883 (2003).
- ²²R.A. Ribeiro, S.L. Bud'ko, C. Petrovic, and P.C. Canfield, *Physica C* **385**, 16 (2003).
- ²³A.A. Golubov, J. Kortus, O.V. Dolgov, O. Jepsen, Y. Kong, O.K. Andersen, B.J. Gibson, K. Ahn, and R.K. Kremer, *J. Phys.: Condens. Matter* **14**, 1353 (2002).
- ²⁴A. Bussmann-Holder and A. Bianconi, *Phys. Rev. B* **67**, 132509 (2003).
- ²⁵F. Giubileo, D. Roditchev, W. Sacks, R. Lamy, D.X. Thanh, J. Klein, S. Miraglia, D. Fruchart, J. Marcus, and Ph. Monod, *Phys. Rev. Lett.* **87**, 177008 (2001).
- ²⁶R.S. Gonnelli (unpublished).
- ²⁷S.C. Erwin and I.I. Mazin, cond-mat/0304456 (unpublished).
- ²⁸A.A. Golubov and I.I. Mazin, *Phys. Rev. B* **55**, 15 146 (1997).
- ²⁹H. Schmidt, K.E. Gray, D.G. Hinks, J.F. Zasadzinski, M. Avdeev, J.D. Jorgensen, and J.C. Burley, cond-mat/0303403, *Phys. Rev. B* (to be published).